ISSN 1560-0904, Polymer Science, Series B, 2016, Vol. 58, No. 2, pp. 152–162. © Pleiades Publishing, Ltd., 2016.
Original Russian Text © L.A. Rishina, Y.V. Kissin, S.S. Lalayan, V.G. Krasheninnikov, E.O. Perepelitsina, T.I. Medintseva, 2016, published in Vysokomolekulyarnye Soedineniya. Ser. B, 2016, Vol. 58, No. 2, pp. 136–146.

POLYMERIZATION

A Novel Efficient Ti(O-*iso*-C_3H_7)$_4$-Based Olefin Polymerization Catalyst System

L. A. Rishina[a,*], Y. V. Kissin[b], S. S. Lalayan[a], V. G. Krasheninnikov[a], E. O. Perepelitsina[c], and T. I. Medintseva[a]

[a] *Semenov Institute of Chemical Physics, Russian Academy of Sciences, ul. Kosygina 4, Moscow, 119991 Russia*

[b] *Department of Chemistry and Chemical Biology, Rutgers, The State University of New Jersey, 610 Taylor Rd., Piscataway, NJ 08854, United States*

[c] *Institute of Problems of Chemical Physics, Russian Academy of Sciences, pr. Akademika Semenova 1, Chernogolovka, Moscow oblast, 142432 Russia*

**e-mail: rishina@polymer.chph.ras.ru*

Received April 30, 2015; Revised Manuscript Received October 5, 2015

Abstract—The polymerization of ethylene and propylene and the copolymerization of ethylene and hexene-1 with a Ti(O-*iso*-Pr)$_4$–$AlR_2Cl/MgBu_2$ catalyst system have been studied. The advantages of this system over metallocene and postmetallocene catalysts are high activity, low cost, and ease of synthesis. The resulting polymers and copolymers are characterized by a broad molecular-mass distribution, which reflects the heterogeneity of the active sites with respect to kinetic parameters. As a consequence, the ethylene/hexene-1 copolymers exhibit compositional heterogeneity. The active sites of the system produce copolymers with a pronounced tendency toward alternation of monomer units. The propylene polymerization product is mostly amorphous atactic polypropylene.

DOI: 10.1134/S1560090416020056

INTRODUCTION

Titanium alkoxides $Ti(OR)_4$ are commonly used for the synthesis of multidentate complexes of titanium that are used as postmetallocene catalysts of various types. However, $Ti(OR)_4$ compounds taken alone are not effective olefin polymerization catalysts. In 1955, K. Ziegler discovered that, mixtures of $Ti(OR)_4$ and AlR_3 do not polymerize ethylene but effective dimerize it to butene-1 [1]. The reaction mechanism includes the formation of metallocycles as intermediates [2–4]; it is crucially different from the mechanism of polymerization of alkenes where the incorporation of the double bond of an alkene occurs via the transition metal–carbon bond. In addition, the activity of the combination of $Ti(OR)_4$ and AlR_2Cl in the ethylene polymerization reaction is extremely low; it is completely absent in the case of propylene [5]. However, we have found that the addition of a mixture of AlR_2Cl and a MgR'_2 organomagnesium compound at a molar ratio of [Al]/[Mg] $\geqslant$ 2.5 to $Ti(OR)_4$ leads to the formation of a very active ternary catalyst system of olefin polymerization. In general, a combination of AlR_2Cl and MgR'_2 is a universal cocatalyst for heterogeneous Ziegler–Natta catalysts and metallocene and postmetallocene complexes [6–8].

In this study, the results of a systematic investigation into the catalytic activity of the Ti(O-*iso*-Pr)$_4$–$AlEt_2Cl/MgBu_2$ system in the polymerization of ethylene and propylene and the copolymerization of ethylene and hexene-1 are described.

EXPERIMENTAL

Materials

Polymerization purity grade ethylene and propylene (99.9 vol %) manufactured at the Moscow Refinery were used without further purification. Special purity grade toluene and hexene-1 were refluxed over Na and distilled under argon. Ti(O-*iso*-Pr)$_4$, $AlEt_2Cl$ (0.8 mol/L solution in heptane), and $MgBu_2$ (0.5 mol/L solution in heptane) purchased from Acros were used without further purification.

Polymerization

All the polymerization reactions were carried out in a 200-mL steel reactor equipped with a stirrer. Before the experiments, the reactor was evacuated at the test temperature for 1 h. In the case of polymerization of ethylene and copolymerization of ethylene and hexene-1, the reactor was filled with toluene or

a toluene/hexene-1 mixture; the amount of the liquid phase was 100 mL. After that, $AlEt_2Cl$ and $MgBu_2$ were successively introduced into the reaction mixture. The resulting mixture was saturated with ethylene; after that, ampule with Ti(O-*iso*-Pr)$_4$ was broken inside the reactor. During the experiments, the pressure in the reactor was maintained constant (4.1 atm); the consumption of ethylene was compensated via feeding from a calibrated vessel. The concentration of ethylene and hexene-1 in the solution was determined with a computer program for the calculation of thermodynamic equilibrium in multicomponent mixtures of hydrocarbons.

Propylene polymerization was conducted via complete filling of the reactor with a liquid monomer as described in [9].

The resulting polymers and copolymers were exposed to a mixture of ethyl alcohol and HCl (10% solution) and then repeatedly washed with water and alcohol and dried to constant masses.

The catalyst activities in ethylene polymerization reactions were estimated from the effective polymerization rate constant $k_{eff} = v_{pol}/(C_E C_{Ti})$ (L/(mol Ti min)), where v_{pol} is the polymerization rate (mol/(L min)) and C_E and C_{Ti} are the concentrations of ethylene and Ti(O-*iso*-Pr)$_4$ (mol/L), and from the polymer yield per mole of Ti(O-*iso*-Pr)$_4$ (kg/mol Ti). The catalyst activities in ethylene polymerization reactions at different temperatures were compared according to the yield with respect to moles of Ti(O-*iso*-Pr)$_4$ and with respect to ethylene concentration [kg/(mol Ti C_E)].

Analysis of Polymers

Gel permeation chromatograms of the polymers were recorded on a Waters GPCV-2000 instrument equipped with a PL-gel column (5 μ, Mixed-C, 300 mm × 7.5 mm) and a refractometer. Analysis of the polymers was conducted in 1,2,4-trichlorobenzene at 135°C and an elution rate of 1 mL/min. The average molecular masses of the products were calculated from a universal calibration curve with the use of PS standards with a narrow molecular-mass distribution (MMD); for PS, $K = 2.80 \times 10^{-4}$ and $\alpha = 0.64$; for PE, $K = 6.14 \times 10^{-4}$ and $\alpha = 0.67$. The procedure for the separation of GPC curves into curves of individual Flory components (polymer products produced by one type of active site) was described in [10, 11].

^{13}C NMR spectra of the polymers (5% solutions in *o*-dichlorobenzene) were recorded at 110°C on a Bruker Avance-400 spectrometer (frequency, 100.613 MHz; relaxation time, 15 s; number of recordings, 500–2000). The assignment of signals in the ^{13}C NMR spectra of the ethylene/hexene-1 copolymers and the polypropylene (PP) was conducted in accordance with data from [12–16]. The IR spectra of the polyethylene (PE) and the copolymers were recorded on a Bruker Tensor 27 FTIR spectrophotometer.

The hexene-1 contents in the copolymers, C_H^{copol} (mol %), were determined from the ^{13}C NMR and IR spectroscopy data according to the ratios of absorbance of the bands at 1380, 1368, and 722 cm^{-1} (D_{1380}/D_{1368} and D_{1380}/D_{722}) with the use of calibration curves [17].

The DSC melting curves of the polymers (samples with masses of 3–5 mg) were recorded on a Netzsch DSC 209-F1 analyzer at a heating rate of 10 K/min. The compositional and structural heterogeneity of the copolymers was analyzed in detail with the use of the data derived during the second melting of the samples at a heating rate of 2 K/min after slow crystallization at a rate of 0.5 K/min beginning from 140°C.

The deformation behavior of the polymers subjected to uniaxial tension was studied with an Instron-1122 machine at rates of extension of 20 mm/min for the PE and copolymer samples and 50 mm/min for the PP. Bilateral blades with a working area of 35 mm × 5 mm were cut from 1-mm-thick plates prepared via hot pressing under a pressure of 10 MPa at 160 (PE, copolymers) and 190°C (PP). The results of determination of elastic modulus E, yield strength σ_y, respective yield elongation ε_y, minimum stress after necking σ_{min}, minimum stress after elongation ε_{min}, ultimate strength σ_u, and ultimate elongation ε_u were averaged over 10 to 14 samples. The measurement error did not exceed 10% for E and σ_u and 20% for ε_u. Residual elongation ε_{res} was calculated as $\varepsilon_{res} = (L_1 - L_o)/L_o \times 100\%$, where L_1 is the sample length after unloading at an elongation of 100% and L_o is the initial sample length.

RESULTS AND DISCUSSION

Homo- and Copolymerization of Olefins over the Ti(O-iso-Pr)$_4$–$AlEt_2Cl$/$MgBu_2$ Catalyst System

Ethylene polymerization. Table 1 shows the ethylene polymerization conditions and the main results. The use of a combination of Ti(O-*iso*-Pr)$_4$ and $AlEt_2Cl$ (without $MgBu_2$) leads to the formation of only traces of the polymer; this result is in agreement with previously published data [1, 5]. However, the addition of $MgBu_2$ at a molar ratio of $[AlEt_2Cl]/[MgBu_2] \sim 3$ results in a sharp increase in the PE yield: At 50°C, it was ~1.5 t/mol Ti or ~3.6 t/(mol Ti C_E).

The ethylene polymerization kinetics exhibits a pronounced nonsteady-state behavior (Fig. 1). At 50°C, about 60% of the total polymer product is formed in the first 10 min, while effective polymerization rate constant k_{eff} decreases about 65-fold over 60 min.

Table 1. Ethylene polymerization over the Ti(O-*iso*-Pr)$_4$–AlEt$_2$Cl/MgBu$_2$ system

T_{pol}, °C	C_E, mol/L	[Ti] × 10^5, mol	[Al] × 10^3, mol	[Mg] × 10^3, mol	Polymer yield		
					g	kg/mol Ti	kg/(mol Ti C_E)
50	0.41	2.36	7.91	0	trace	–	–
30	0.50	1.78	5.65	1.75	9.3	520	1040
40	0.44	1.17	4.07	12.5	9.2	790	1790
50	0.41	0.62	2.26	0.75	9.0	1460	3570

Polymerization in toluene; liquid phase volume, 100 mL; overall reactor pressure, 4.1 atm; reaction time, 1 h.

Table 2. Copolymerization of ethylene and hexene-1 over the Ti(O-*iso*-Pr)$_4$–AlEt$_2$Cl/MgBu$_2$ system*

C_E^{mon}, mol/L	C_H^{mon}, mol/L	[Ti] × 10^5, mol	[Al]/[Ti], mol/mol	[Al]/[Mg], mol/mol	Yield, kg/mol Ti	C_H^{copol}, mol %**
0.42	0	0.62	370	3.0	1480	0
0.42	0.25	0.80	290	3.0	940	0.9
0.43	0.60	0.84	320	3.2	840	1.3
0.44	0.90	0.84	320	3.2	2430	8.4
0.44	1.50	0.79	290	3.0	3010	15.8

*Temperature, 50°C; liquid phase volume, 100 mL; total reactor pressure, 4.1 atm; reaction time, 1 h.
**^{13}C NMR data.

According to IR spectroscopy, the resulting PE is a linear polymer: The spectra of the samples do not exhibit absorption bands of methyl groups in the branches (1378 cm^{-1}).

Copolymerization of ethylene and hexene-1. The Ti(O-*iso*-Pr)$_4$–AlEt$_2$Cl/MgBu$_2$ catalyst system was efficient also for the synthesis of ethylene/hexene-1 copolymers (Table 2). In the presence of this system, copolymers with a hexene-1 content (C_H^{copol}) from ~1 to ~15 mol % were synthesized. At 50°C, the copolymer yield lies in the range 0.85–3.0 t/(mol Ti h), depending on the composition of the monomer mixture. At a molar ratio of hexene-1 and ethylene 0.6 and 1.4, the activity of the system decreases. However, a further increase in the hexene-1 concentration leads to a significant activation of the catalyst: In these cases, the copolymer yield is 1.5–2.0 times higher than that in the ethylene polymerization.

This increase in catalyst activity in ethylene polymerization reactions with the addition of α-olefins is well known both for heterogeneous Ziegler–Natta and chromium oxide catalysts and for metallocene and postmetallocene catalysts [11, 18–20].

There are two alternative explanations for this phenomenon. The first is based on a purely mechanical effect: the polymer molecules surrounding the active sites can act as a diffusion barrier to ethylene, which is lower in the case of copolymers with lower degrees of crystallinity. In fact, the degrees of crystallinity of the copolymers prepared at a high hexene-1 concentration (the last two examples in Table 2, C_H^{copol} of ~8 and ~16 mol %, respectively) are significantly lower than the degree of crystallinity of the PE (Table 3).

The second explanation involves a chemical mechanism [18, 20]. This mechanism is based on the fact that the rate constant for the incorporation of ethylene into the Ti–C bond in the Ti–CH_2–CH_3 active site at each stage of the polymer-chain initiation is lower than the rate constant of the incorporation of ethylene in the case of the Ti–$(CH_2–CH_2)_n$–C_2H_5 active site at all subsequent stages of chain propagation. The reason for the relative inertness of the Ti–CH_2–CH_3 site is a stronger agostic interaction between its β-CH_3 group and the Ti atom compared to the agostic interaction between the β-CH_2 group and the Ti atom in the Ti–CH_2–CH_2–polymer sites. In the presence of α-olefin CH_2=CH–*R* (in the case of hexene-1, *R* = C_4H_9), the Ti–CH_2–CH_3 initiation site is partially replaced with the Ti–CH_2–CH_2–*R* site into which ethylene is incorporated at the same rate constant as that for the incorporation of ethylene into the Ti–CH_2–CH_2–polymer site.

A "comonomer" effect is characteristic of any copolymerization reactions of ethylene and α-olefins, including high-temperature reactions in solutions and reactions involving nonreactive α-olefins [19, 20], that is in better agreement with the chemical explanation.

Comparison of the compositions of the monomer mixture and the copolymer (Table 2) provides an approximate estimate of the effective reactivity ratio $r_1 = k_{E–E}/k_{E–H} \sim (C_E/C_H)^{copol}/(C_E/C_H)^{mon}$, where $k_{E–E}$ and $k_{E–H}$ are the rate constants for the addition of eth-

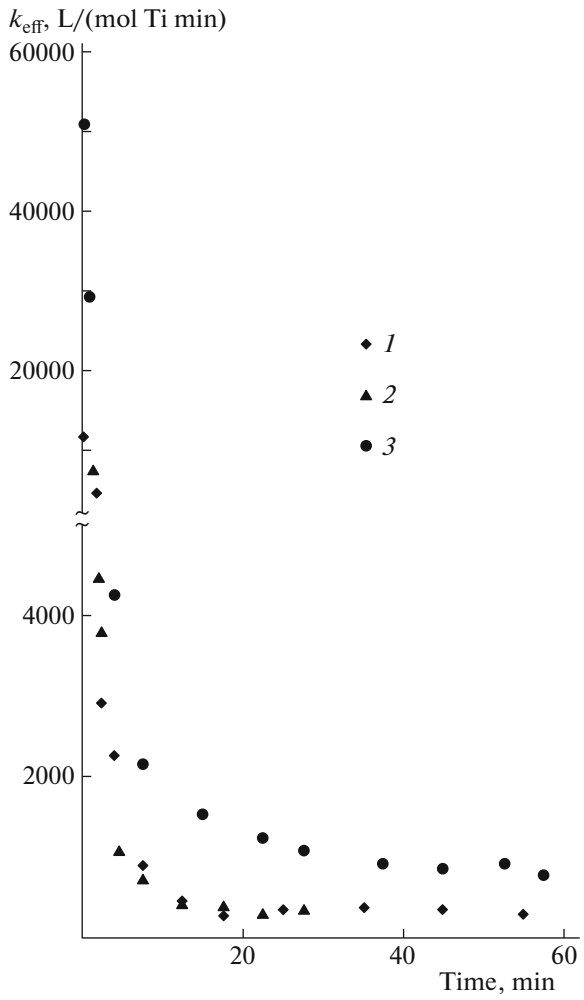

Fig. 1. Kinetic curves of ethylene polymerization at (*1*) 30, (*2*) 40, and (*3*) 50°C.

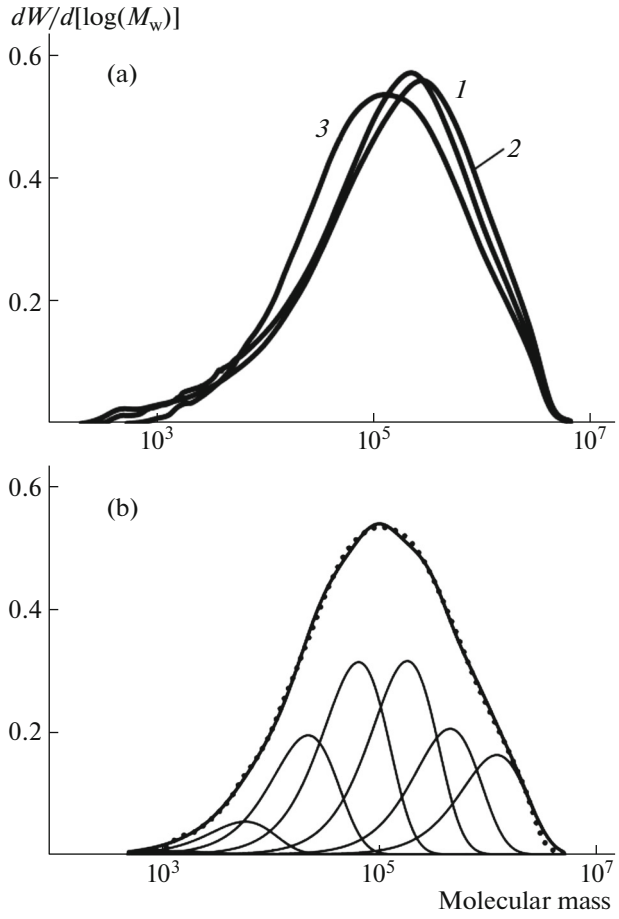

Fig. 2. (a) GPC curves of (*1*) the PE and (*2, 3*) the copolymers with C_H^{copol} = (*2*) 1.3 and (*3*) 8.4 mol % and (b) separation of the GPC curve of the copolymer with C_H^{copol} = 8.4 mol % into the Flory components. The points and the lines denote experimental and calculated data, respectively.

ylene and hexene-1 to the growing polymer chain with the last ethylene unit, >Ti–CH_2–CH_2–polymer. At a low hexene-1 concentration in the reaction mixture, the r_1 value is fairly high: ~60 (that is, the reactivity of ethylene is 60 times higher than that of hexene-1.) As the hexene-1 concentration increases, the r_1 value decreases to 30. This change can be attributed to the multicenter nature of the catalyst, which is discussed below. The introduction of hexene-1 leads to the activation of additional active sites that exhibit a higher reactivity toward hexene-1 than that of the active sites formed in the presence of only ethylene.

Molecular-mass heterogeneity and compositional heterogeneity of PE and the ethylene/hexene-1 copolymers. The data listed in Table 3 show that increase in the hexene-1 contents in the copolymers lead to decrease in the molecular masses and effective melting temperatures T_m of the copolymers and to sharp decrease in melting heats ΔH_m and degrees of crystallinity χ. These features are typical for the copolymerization of ethylene and α-olefins in general [11, 20].

According to GPC data, both the PE and the ethylene/hexene-1 copolymers have broad MMDs, an outcome that suggests the catalyst contains different types of active sites responsible for the formation of macromolecules with different average molecular masses (Fig. 2a). Figure 2b and Table 4 show the results of the separation of the MMD curves into Flory components.

Analysis of the results suggests that the introduction of hexene-1 into the polymerization medium leads to two effects: a decrease in the M_w value of each Flory component and an increase in the fraction of active sites that provide the formation of macromolecules with relatively low molecular masses (Flory components III and IV).

Table 3. Molecular-mass and structural characteristics of the PE and the ethylene/hexene-1 copolymers

C_H^{copol}, mol %	$M_w \times 10^{-3}$	M_w/M_n	T_m^*, °C	ΔH_m^*, J/g*	χ, %**
0	446	24	133	190	65
0.9	369	25	128	135	46
1.3	400	19	127	125	43
8.4	354	11	123	44	15
15.8	142	20	–	16	~6

*Heating rate, 2 °C/min, second melting.
**Degree of crystallinity according to DSC, $\chi = (\Delta H_m/\Delta H_m^0) \times 100$, where $\Delta H_m^0 = 293.0$ J/g.

Table 4. Results of separation of the GPC curves of the PE and the ethylene/hexene-1 copolymers synthesized at 50°C*

Flory component	$M_w \times 10^{-3}$	Content, %	$M_w \times 10^{-3}$	Content, %	$M_w \times 10^{-3}$	Content, %	$M_w \times 10^{-3}$	Content, %
	$C_H^{copol} = 0$ mol %		$C_H^{copol} = 1.3$ mol %		$C_H^{copol} = 8.4$ mol %		$C_H^{copol} = 15.8$ mol %	
I	1.8	2.1	1.8	2.0	1.6	0.4	2.0	7.4
II	7.6	4.3	7.2	5.6	6.7	4.3	7.5	17.4
III	28	10.8	27	10.4	26	15.6	23	27.0
IV	86	19.1	81	19.1	77	25.0	60	22.6
V	254	29.0	225	29.9	222	25.3	175	15.2
VI	660	20.4	600	20.0	550	16.4	570	7.4
VII	1700	14.3	1600	13.0	1600	13.0	1600	3.0
Average values**	$M_w^{av} \times 10^{-3} = 470$		$M_w^{av} \times 10^{-3} = 418$		$M_w^{av} \times 10^{-3} = 363$		$M_w^{av} \times 10^{-3} = 1388$	
	$M_w/M_n = 24$		$M_w/M_n = 22$		$M_w/M_n = 14.5$		$M_w/M_n = 21$	

*The synthesis conditions for the PE and the copolymers are given in Tables 1 and 2.
**Calculated from the M_w values of the Flory components and their content.

The presence of different types of active sites makes it possible to assume that the macromolecules differ not only in molecular-mass characteristics but also in composition [11].

This assumption was verified through the DSC method. It was previously shown that the melting temperatures of ethylene/α-olefin copolymers and the shapes of the DSC melting curves depend on the compositions and degrees of compositional heterogeneity of the copolymers [20]. Copolymers synthesized over single site metallocene catalysts exhibit relatively narrow melting peaks, while the melting peaks of copolymers prepared in the presence of multicenter heterogeneous Ziegler–Natta catalysts are broader. It is evident from Fig. 3 that an increase in the hexene-1 content leads to a change in the shape of the melting curve and a rapid decrease in melting heat ΔH_m (see also Table 3).

Compositional heterogeneity is particularly pronounced in the case of the copolymer with $C_H^{copol} =$ 8.4 mol %, whose amorphous fraction is 85% (Fig. 3, Table 3). In addition, it contains two small low crystallinity components. One exhibits a broad melting peak at ~100°C (according to [20], it contains ~4 mol % of hexene-1); the other component exhibits a weak melting peak at ~123°C ($C_H^{copol} \sim 1.7$ mol %). In addition, the melting peaks of the copolymers with $C_H^{copol} = 0.9$ and 1.3 mol % are slightly broader than the melting peak of the PE; this fact indicates the presence of copolymer components with different hexene-1 content and T_m values.

This statement is confirmed by the results of simulation the melting curves of copolymers via the method described in [20]. For example, Fig. 4 shows the results of simulation of the melting curve of the copolymer with $C_H^{copol} = 1.3$ mol %, which suggest that this product is a mixture of five components with different compositions.

Microstructuring of the copolymers. Figure 5 shows the ^{13}C NMR spectrum of the ethylene/hexene-1 copolymer with $C_H^{copol} = 15.8$ mol % in the region of 22–42 ppm, which exhibits signals of all the protons of the ethylene and hexene-1 units except that of the methyl group, which occurs at 14.1 ppm. The assignment of signals was conducted according to [12]. The results—strong signals of triads CH(EHE) at

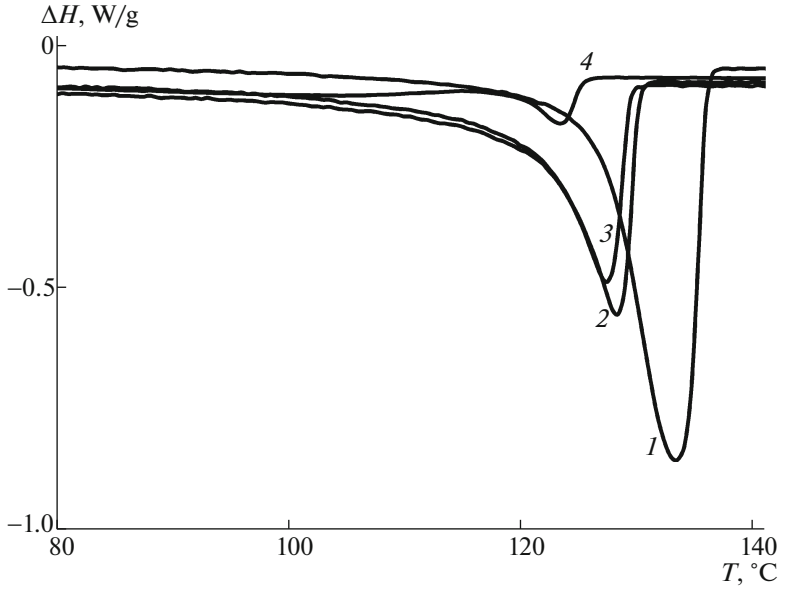

Fig. 3. DSC melting curves of (*1*) the PE and (*2–4*) the ethylene/hexene-1 copolymers with C_H^{copol} = (*2*) 0.9, (*3*) 1.3, and (*4*) 8.4 mol %.

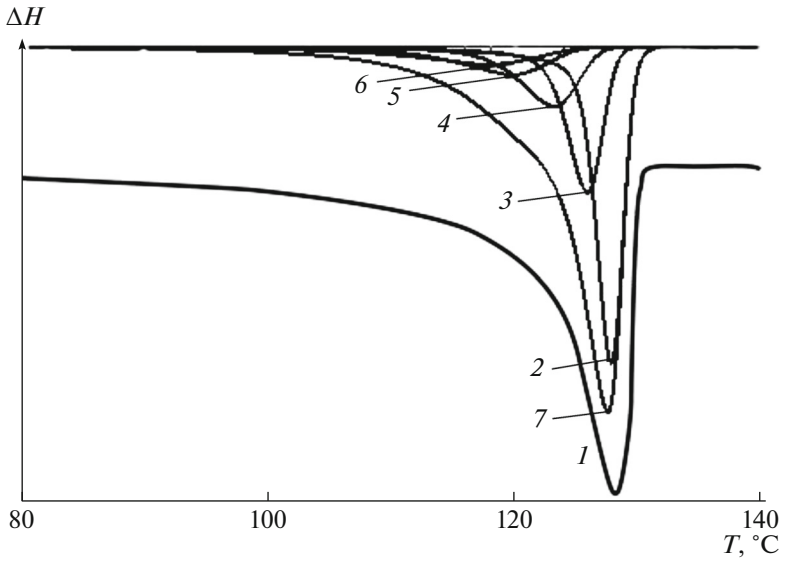

Fig. 4. (*1*) Experimental DSC melting curve of the ethylene/hexene-1 copolymer with C_H^{copol} = 1.3 mol %; (*2–6*) the separation of the curve into components with C_H^{copol} = (*2*) 1.2, (*3*) 1.5, (*4*) 1.8, (*5*) 2.2, and (*6*) 2.5 mol %; the relative contents of the components are 0.41, 0.24, 0.16, 0.11, and 0.09, respectively; (*7*) the sum of curves *2–6*.

38.1 ppm, triads 3B(EHE) at 29.5 ppm, and tetrads β,δ$^+$-CH_2(EHEE) at 27.3 ppm—suggest that hexene-1 is mostly in the form of isolated monomer units (H) in the EHE sequences (see the strong signals of triads CH(EHE) at 38.1 ppm, triads 3B(EHE) at 29.5 ppm, and tetrads β,δ$^+$-CH_2(EHEE) at 27.3 ppm). Only a slight fraction of the monomer units of hexene-1 is in HH dyads: tetrads α,α-CH_2(EHHE) at 40.1 ppm, tetrads β,δ$^+$-CH_2(HHEE) at 27.1 ppm, triads CH(EHH) at 35.7 ppm, and triads 3B(EHH) at 29.3 ppm.

The ability of the active sites to alternate monomer units can be estimated from the product of reactivity ratios r_1r_2, where $r_1 = k_{E-E}/k_{E-H}$ and $r_2 = k_{H-H}/k_{H-E}$ [20]. If $r_1r_2 = 1$, the relative probability of occurrence

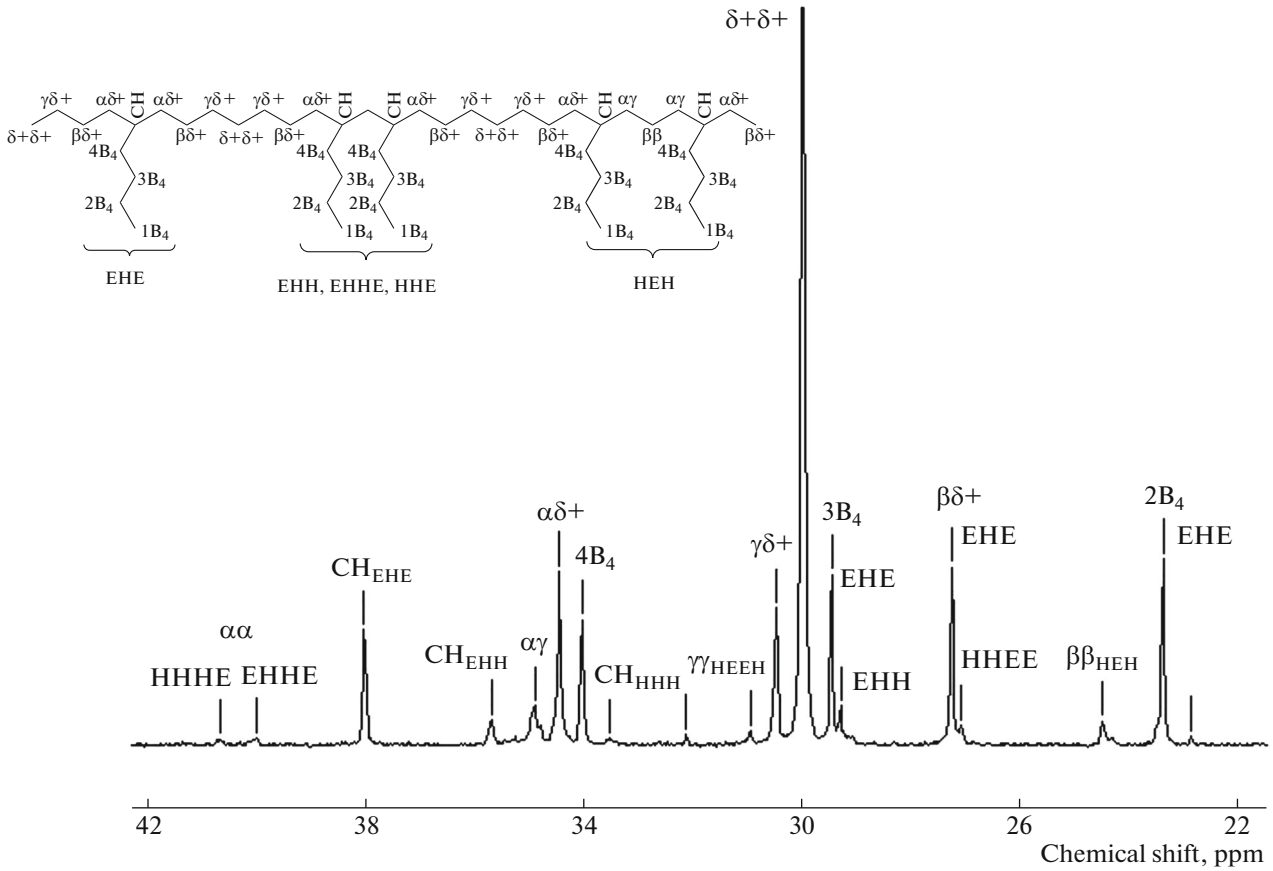

Fig. 5. Fragment of the ^{13}C NMR spectrum of the ethylene/hexene-1 copolymer with C_H^{copol} = 15.8 mol % and the assignment of signals.

of a given monomer in the chain depends only on the monomer content in the copolymer, not on the nature of the preceding monomer unit (random copolymers). If $r_1r_2 < 1$, the catalyst exhibits a tendency to alternate monomer units in the copolymer chains (alternating copolymers); in the limit at $r_2 = 0$, hexene-1 is present in the copolymer chains only in the form of isolated units.

^{13}C NMR spectra are the most sensitive tool to determine r_1r_2. This value can be found via comparison of the relative intensities of the signals of the blocks of hexene-1, EHH and EHHE, and the signal of the isolated hexene-1 units, EHE, or the signal of the isolated ethylene units, HEH.

Expressions required for calculating the contents of the EHH, EHHE, EHE, and HEH sequences as functions of copolymer compositions C_H^{copol} and r_1r_2 values are known from the literature [11]. The [EHHE]/[HEH] and [EHH]/[HEH] ratios are convenient for estimation of the r_1r_2 value because they are not particularly sensitive to the composition of a copolymer:

$$[EHH]/[HEH] = 2r_1r_2(1 + IN)/(r_1r_2 + IN), \quad (1)$$

$$[EHHE]/[HEH] = r_1r_2IN(1 + IN)/(r_1r_2 + IN)^2, \quad (2)$$

where $IN = 0.5\{f - 1 + [(f - 1)^2 + 4r_1r_2f]^{0.5}\}$ and $f = C_E^{copol}/C_H^{copol} = (100 - C_H^{copol})/C_H^{copol}$.

For the ethylene/hexene-1 copolymer at C_H^{copol} = 15.8 mol %, [EHH]/[HEH] ~ 0.91 and [EHHE]/[HEH] ~ 0.34. In this case, the r_1r_2 values calculated from Eqs. (1) and (2) via the program Mathematics 8 lie in the range 0.35–0.45. These r_1r_2 values suggest that the active sites of the studied catalyst system exhibit a tendency toward alternation of monomer units in the chains.

Propylene polymerization. It was previously shown that the Ti(O-*iso*-Pr)$_4$–AlEt$_2$Cl/MgBu$_2$ system provides efficient polymerization of propylene [21]; in the case of polymerization in a liquid monomer, the PP yield is ~10 t/mol Ti h (Table 5). The resulting polymers are characterized by $M = (50–100) \times 10^3$ and a broad MMD. In these polymers, the content of the amorphous fraction soluble in boiling heptane is more than 80%. The boiling heptane insoluble fraction contains also ~50% amorphous atactic PP with a higher molecular mass.

Table 5. Propylene polymerization over the Ti(O-*iso*-Pr)$_4$–$AlEt_2Cl/MgBu_2$ catalyst system [23]*

T_{pol}, °C	C_{Pr}, mol/L	[Ti] × 10^5, mol	[Al]/[Ti], mol/mol	[Al]/[Mg], mol/mol	Yield, kg/mol Ti	Amorphous fraction, %**	$M_w \times 10^{-3}$	M_w/M_n
30	11.9	1.42	220	3.4	2250	82.5	50.9	4.2
40	11.4	1.00	350	3.5	5000	84.7	87.7	6.9
50	11.2	0.62	350	3.5	9680	86.2	98.4	8.1

*Polymerization in liquid propylene; reaction time, 1 h.
**Boiling heptane soluble fraction.

Table 6. Signals of the CH_3 groups in the ^{13}C NMR spectrum of the boiling heptane soluble fraction of the PP

Triads *mm*			Triads *mr*			Triads *rr*		
pentads	chemical shift, ppm	content, %	pentads	chemical shift, ppm	content, %	pentads	chemical shift, ppm	content, %
mmm	21.30	21.4	*mmrr*	20.50	14.7	*rrrr*	19.76–19.84	4.4
mmmr	21.02	14.1	*mmrm*	20.28	26.8	*mrrr*	19.54–19.61	5.8
			+ *rrmr*			*mrrm*	19.30–19.46	5.0
rmmr	20.76	4.0	*rmrm*	20.0–20.1	~2.7			

The PP was prepared in liquid propylene at 50°C.

As an example, Fig. 6 shows the ^{13}C NMR spectrum (region of signals of methyl groups) of the boiling heptane soluble fraction of PP and the spectral resolution into signals of various stereo-sequences. The position of each signal and the relative contents of stereo-sequences are listed in Table 6. The ^{13}C NMR data suggest that this fraction mostly has a head-to-tail structure [21]; the $T_{\alpha\gamma}$ and $T_{\beta\gamma}$ signals of regio-errors at about 38 and 31 ppm [22] are fairly low. The polymer is almost atactic: it contains all the possible stereo-sequences in comparable amounts. The distribution of stereo-sequences in this sample is similar to the distribution characteristic for the soluble fractions of the PP prepared with the use of supported titanium–magnesium catalysts [23–25]. For instance, along with irregular sequences, the amorphous fraction contains a certain amount of isotactic pentads; the [*mmmm*] value is ~0.21 (Fig. 6).

Atactic PP is an important commercial product; it is used to manufacture construction adhesives, filler pastes, sealing mastics, road pavement, and adhesive films [25–26]. The possibility of targetedly synthesiz-

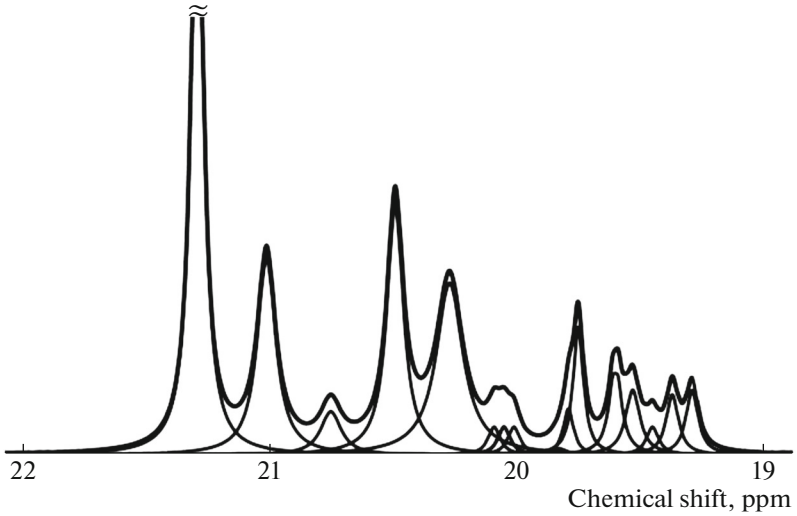

Fig. 6. ^{13}C NMR spectrum of the boiling heptane soluble fraction of the PP (derived at 50°C) in the region of signals of methyl groups and the spectral resolution into signals of various stereo-pentads and heptads (see Table 6).

Table 7. Mechanical properties of the polymers

Sample	E, MPa	σ_y, MPa	ε_y, %	σ_{min}, MPa	ε_{min}, %	σ_u, MPa	ε_u, %	ε_{res}, %
PE	890	24.1	12.6	20.3	77	30	385	80
Amorphous PP	16	–	–	–	–	2.3	550	25
Ethylene/hexene-1 copolymer	12	–	–	–	–	0.9	80	–

ing amorphous PP with the use of the Ti(O-*iso*-Pr)$_4$–AlEt$_2$Cl/MgBu$_2$ system is of practical interest.

Mechanical Properties of the Polymers

Figure 7 shows the uniaxial stress–strain diagrams of the PE, PP, and ethylene/hexene-1 copolymer with C_H^{copol} = 15.8 mol % that were synthesized in this study.

The resulting PE is a typical semicrystalline HDPE [27]; the stress–strain curve exhibits yield strength σ_y and an extended necking region with $\sigma_{min} \sim 0.85\ \sigma_y$, after which the polymer undergoes uniform strain hardening. The deformation behaviors of the atactic PP and the copolymer are different: Deformation occurs without necking. Unlike isotactic PP, whose deformation is similar to that of PE, amorphous PP does not have a yield point; the linear region of elongation of the PP ends at $\varepsilon \sim 0.7\%$; after that, the stress nonlinearly increases to a limiting value. The patterns of deformation of the ethylene/hexene-1 copolymer and the PP are similar; differences are observed only in the ultimate-strength and ultimate-elongation values. These stress–strain diagrams are typical for elastomeric materials [27].

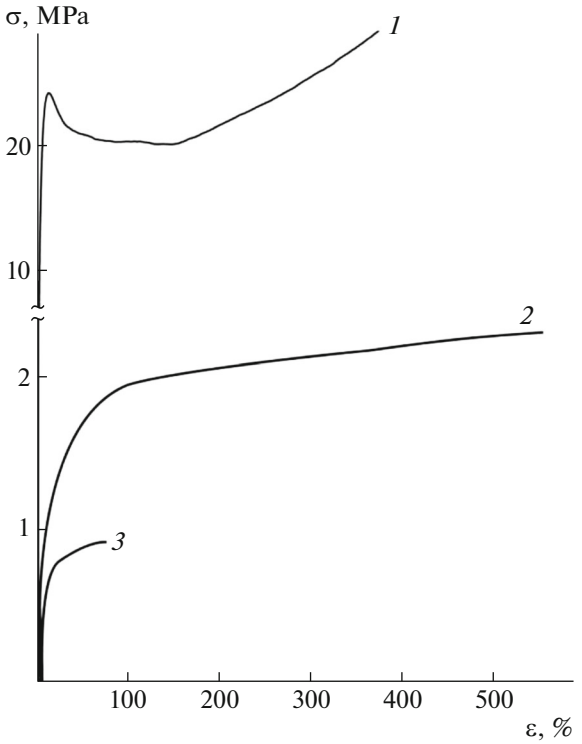

Fig. 7. Uniaxial stress σ–strain ε diagrams for (*1*) the PE, (*2*) the amorphous PP, and (*3*) the ethylene/hexene-1 copolymer with C_H^{copol} = 15.8 mol %.

Atactic PP has low values of elastic modulus E and ultimate strength σ_u, while maintaining a high value of ultimate elongation ε_u (Table 7). Residual elongation ε_{res} for the PP is 25%. The elastic modulus of the amorphous ethylene/hexene-1 copolymer ($\chi \sim 5\%$) is comparable with that of the amorphous PP ($\chi \sim 7\%$); however, the ultimate-strength and ultimate-elongation values are significantly lower.

Thus, the mechanical properties of the amorphous PP and the ethylene/hexene-1 copolymer prepared over the Ti(O-*iso*-Pr)$_4$–AlEt$_2$Cl/MgBu$_2$ catalyst system are similar to those of elastomeric materials. Polymers of this type can be used in composites with rigid plastics in order to increase the elasticity and improve the mechanical characteristics of these materials.

Chemical Aspects of the Ti(O-iso-Pr)$_4$–AlEt$_2$Cl/MgBu$_2$ Catalyst System

Both previously published data [1, 5] and our results (Table 1) show that combinations of Ti(OR)$_4$ and such organoaluminum compounds as AlR$_2$Cl or AlR$_3$ are not olefin polymerization catalysts. However, owing to the addition of MgR'$_2$, combinations of Ti(OR)$_4$ and AlR$_2$Cl become highly active catalysts.

Reactions between Ti(OR)$_4$ and organoaluminum compounds were described in detail previously [28–31]. These reactions lead to the alkylation of Ti(OR)$_4$ to (RO)$_3$Ti^{IV}–R and (RO)$_2$Ti^{IV}R$_2$; the reduction of these compounds to Ti^{III}(RO)$_3$ and (RO)$_2$Ti^{III}–R; and the formation of Ti^{III} complexes with AlR$_2$(OR) or AlR(OR)Cl, such as [Ti^{III}(OR)$_3$]2AlR$_2$(OR), [Ti^{III}(OR)$_3$]AlR$_2$(OR), and [(RO)$_2$Ti^{IV}–R]AlR(OR)Cl.

The active sites of olefin polymerization are cationic complexes of Ti^{IV} or Ti^{III} that contain a Ti$^+$–C bond [11]. The efficiency of combinations of AlR$_2$Cl and MgBu$_2$ in the formation of these complexes can be most probably attributed to two factors. First, AlEt$_2$Cl

and $MgBu_2$ rapidly react to form highly dispersed $MgCl_2$, with the Lewis-acidic surface [6, 8]:

$$MgBu_2 + 2AlEt_2Cl \rightarrow [MgCl_2] + 2AlEt_2Bu. \quad (3)$$

The cocatalyst used in this study was prepared at $[AlEt_2Cl]/[MgBu_2] > 3$ (Tables 1, 2). Ti(O-*iso*-Pr)$_4$ is added to the mixture at the last stage of catalyst preparation; it can react with both excess $AlEt_2Cl$ and $AlEt_2Bu$. Once the $(RO)_3Ti^{IV}$–R and $(RO)_2Ti^{III}$–R products or their complexes with organoaluminum compounds are adsorbed on the acidic surface of $MgCl_2$, they can be ionized to form Ti^+–C polymerization sites on the $MgCl_2$ surface:

$$\begin{gathered}(RO)_3Ti{-}R + [MgCl_2] \\ \rightarrow [(RO)_2Ti^+{-}R]_{ads}/[MgCl_2\cdots OR]^-,\end{gathered} \quad (4)$$

$$\begin{gathered}(RO)_2Ti{-}R + [MgCl_2] \\ \rightarrow [(RO)Ti^+{-}R]_{ads}/[MgCl_2\cdots OR]^-.\end{gathered} \quad (5)$$

The second possible cause is the formation of the contact ion pairs $[MgBu]^+[Et_2Bu_2Al]^-$ and $[MgBu]^+[EtBuAlCl\cdots AlBuEt_2]^-$ from $MgBu_2$ or MgBuCl (the intermediate in reaction (3)) [6, 8]. These ion pairs can convert $(RO)_3Ti^{IV}$–R or $(RO)_2Ti^{III}$–R into active sites of an other type: for example,

$$\begin{gathered}(RO)_3Ti{-}R + [MgBu]^+[Et_2Bu_2Al]^- \\ \rightarrow [(RO)_2Ti^+{-}R][Et_2Bu_2Al]^- + MgBu(OR).\end{gathered} \quad (6)$$

$Ti(OR)_4$–$AlR_2Cl/MgBu_2$ catalysts contain active sites of various types, which differ in both kinetic parameters (they produce polymer fractions with different M_w values) and copolymerization ability. It can be assumed that these active sites are formed from different compounds of $(RO)_xTi$–R and $(RO)_yTiR_2$ that contain both Ti^{IV} and Ti^{III}.

CONCLUSIONS

The Ti(O-*iso*-Pr)$_4$–$AlEt_2Cl/MgBu_2$ system is an effective catalyst for the polymerization of ethylene and propylene and the copolymerization of ethylene and hexene-1. The advantages of this system over metallocene and postmetallocene catalysts are high activity, low cost, and ease of synthesis. All components of the system are commercial products soluble in aromatic and aliphatic hydrocarbons. The reaction products are linear PE, amorphous generally atactic PP, and ethylene/hexene-1 copolymers containing from 1 to 16 mol % hexene-1. Each of the resulting polymers is characterized by a broad MMD, which represents the heterogeneity of the active sites with respect to kinetic parameters. In addition, the ethylene/hexene-1 copolymers exhibit compositional heterogeneity. The active sites of the system have a pronounced tendency toward alternation of monomer units in the copolymer chains.

ACKNOWLEDGMENTS

The authors thank K.P. Brylyakov for ^{13}C NMR analysis of the polymers.

This work was supported by the Russian Foundation for Basic Research (project nos. 13-03-00296 and 13-03-00948).

REFERENCES

1. K. Ziegler and H. Martin, US Patent No. 2943125 (1960).
2. G. Lefebre and Y. I. Chauvin, in *Aspects of Homogeneous Catalysis*, Ed. by R. Ugo (Carlo Manfredi, Mila, 1970), Chap. 3, pp. 107–201.
3. S. M. Pillai, G. L. Tembe, M. Ravindranathan, and S. Sivaram, Ind. Eng. Chem. Res **27**, 1971 (1988).
4. D. L. Beach and Y. V. Kissin, J. Polym. Sci., Polym. Chem. Ed. **22** (11), 3027 (1984).
5. L. Kollar, H. Schnecko, and W. Kern, Makromol. Chem. **142**, 21 (1971).
6. Y. V. Kissin, R. I. Mink, A. J. Brandolini, and T. E. Nowlin, J. Polym. Sci., Part A: Polym. Chem. **47** (13), 3271 (2009).
7. Y. V. Kissin, T. E. Nowlin, R. I. Mink, and A. J. Brandolini, Macromolecules **33** (12), 4599 (2000).
8. L. A. Rishina, N. M. Galashina, S. C. Gagieva, V. A. Tuskaev, and Y. V. Kissin, Eur. Polym. J. **49** (1), 147 (2013).
9. L. A. Rishina, N. M. Galashina, S. C. Gagieva, V. A. Tuskaev, B. M. Bulychev, and Y. N. Belokon, Polym. Sci., Ser. A **50** (2), 110 (2008).
10. Y. V. Kissin, J. Polym. Sci., Part A: Polym. Chem. **33** (2), 227 (1995).
11. Y. V. Kissin, *Alkene Polymerization Reactions with Transition Metal Catalysts* (Elsevier, Amsterdam, 2008).
12. E. T. Hsieh and J. C. Randall, Macromolecules **15** (5), 1402 (1982).
13. T. Hayashi, Y. Inoue, R. Chujo, and T. Asakura, Polymer **29**, 138 (1988).
14. F. S. Schilling and A. E. Tonelli, Macromolecules **13** (2), 270 (1980).
15. V. Busico, R. Cipullo, G. Monaco, M. Vacatello, and A. L. Segre, Macromolecules **30** (20), 6251 (1997).
16. V. Busico, R. Cipullo, G. Monaco, G. Talarico, M. Vacatello, J. C. Chadwick, A. L. Segre, and O. Sudmeijer, Macromolecules **32** (13), 4173 (1999).
17. T. E. Nowlin, Y. V. Kissin, and K. P. Wagner, J. Polym. Sci., Part A: Polym. Chem. **26** (3), 755 (1988).
18. T. E. Nowlin, R. I. Mink, and A. J. Brandolini, J. Polym. Sci., Part A: Polym. Chem. **37** (23), 4255 (1999).
19. M. P. McDaniel, E. D. Schwerdtfeger, and M. D. Jensen, J. Catal. **314**, 109 (2014).
20. Y. V. Kissin, J. Polym. Sci., Part B: Polym. Phys. **49** (3), 195 (2011).
21. Y. V. Kissin, L. A. Rishina, S. S. Lalayan, and V. G. Krasheninnikov, J. Polym. Sci., Part A: Polym. Chem. **53** (18), 2124 (2015).

22. T. Asakura, N. Nakayama, M. Demura, and A. Asano, Macromolecules **25**, 4876 (1992).

23. Y. Doi, E. Suzuki, and T. Keii, Makromol. Chem., Rapid Commun. **2**, 293 (1981).

24. T. Hayashi, Y. Inoue, R. Chujo, and Y. Doi, Polymer **30**, 1714 (1989).

25. J. Karger-Kocsis, *Amorphous or Atactic Polypropylene in Polypropylene* (Springer, Washington, DC, 1999), Vol. 2, p. 7.

26. L. Resconi and R. Silvestri, in *Polymeric Materials Encyclopedia*, Ed. by J. C. Salamone (CRC Press, Boca Raton, FL, 1996), Vol. 9, p. 6609.

27. *Fracture*, Ed. by H. Liebowitz (Academic Press, Washington, DC, 1972), Vol. 7(II).

28. G. Natta, L. Porri, A. Carbonaro, and G. Stoppa, Macromol. Chem. **77**, 114, 126, 216 (1964).

29. D. H. Dawes and C. A. Winkler, J. Polym. Sci., Part A: Polym. Chem. **2** (7), 3029 (1964).

30. T. S. Dzhabiev, F. S. D'yachkovskii, and A. E. Shilov, Vysokomol. Soedin., Ser. A **13** (2), 2474 (1971).

31. I. Ono and T. Keii, J. Polym. Sci., Part A: Polym. Chem. **4** (10), 2441 (1966).

Translated by M. Timoshinina